Characterization of Electronic and Ionic Transport in Li[subscript 1-x]Ni[subscript 0.8]Co[subscript 0.15]Al[subscript 0.05]O[subscript 2](NCA)

Characterization of Electronic and Ionic Transport in $Li_{1-x}Ni_{0.8}Co_{0.15}Al_{0.05}O_2$ (NCA)

Ruhul Amin,[a,*] Dorthe Bomholdt Ravnsbæk,[a,b] and Yet-Ming Chiang[a,*,z]

[a]*Department of Materials Science and Engineering, Massachusetts Institute of Technology (MIT), Cambridge, Massachusetts 02139, USA*
[b]*Department of Physics, Chemistry and Pharmacy, University of Southern Denmark (SDU), 5320 Odense M, Denmark*

Despite the extensive commercial use of $Li_{1-x}Ni_{0.8}Co_{0.15}Al_{0.05}O_2$ (NCA) as the positive electrode in Li-ion batteries, and its long research history, its fundamental transport properties are poorly understood. These properties are crucial for designing high energy density and high power Li-ion batteries. Here, the transport properties of NCA are investigated using impedance spectroscopy and dc polarization and depolarization techniques. The electronic conductivity is found to increase with decreasing Li-content from $\sim 10^{-4}$ Scm^{-1} to $\sim 10^{-2}$ Scm^{-1} over $x = 0.0$ to 0.6, while lithium ion conductivity is at least five orders of magnitude lower for $x = 0.0$ to 0.75. A surprising result is that the lithium ionic diffusivity vs. x shows a v-shaped curve with a minimum at $x = 0.5$, while the unit cell parameters show the opposite trend. This suggests that cation ordering has greater influence on the composition dependence than the Li layer separation, unlike other layered oxides. From temperature-dependent measurements in electron-blocking cells, the activation energy for lithium ion conductivity (diffusivity) is found to be 1.25 eV (1.20 eV). Chemical diffusion during electrochemical use is limited by lithium transport, but is fast enough over the entire state-of-charge range to allow charge/discharge of micron-scale particles at practical C-rates.

Manuscript submitted January 2, 2015; revised manuscript received March 18, 2015. Published March 28, 2015. This was Paper 260 presented at the San Francisco, California, Meeting of the Society, October 27–November 1, 2013.

Cathodes having high energy and power density, adequate safety, excellent cycle life, and low cost are crucial for Li-ion batteries that can enable the commercialization of electric transportation.[1] Towards this end, much research has previously focused on the development of the $LiNi_{1-x}Co_xO_2$ (NC)[2–10] cathode due to its high capacity (~275 mAh/g) and favorable operating cell voltage (4.3 V vs. Li/Li^+), which is within the voltage stability window of current liquid electrolytes. This compound also has lower cost than $LiCoO_2$; but despite extensive optimization, e.g., with respect to the Ni/Co ratio,[2–10] NC still suffers from poor structural stability during electrochemical cycling.[11] Significant efforts were subsequently focused on improving structural stability by doping with small amounts of electrochemically inactive elements such as Al and Mg.[12–17] One of the most promising compositions that emerged is $Li_1Ni_{0.8}Co_{0.15}Al_{0.05}O_2$ (NCA), currently in widespread commercial use. This intercalation material exhibits solid solution behavior during the extraction of lithium[3,4,18] and is structurally stable upon cycling.[2] The majority of studies of NCA have focused on structural and electrochemical characterization. Surprisingly, there is limited, and conflicting, data on the basic transport properties of the NC/NCA family of compounds.[19–23] Cho et al.,[19] and Montoro et al.[20] determined the chemical diffusivity of $LiNi_{1-x}Co_xO_2$ using GITT measurements of composite cathodes (e.g., NC powder combined with polymer binder and carbon additive), and reported results varying over several orders of magnitude. They also reported that the chemical diffusivity of $Li_xNi_{0.8}Co_{0.2}O_2$ is nearly independent of lithium content. In contrast, Montoro et al.[20] found a wider variation of lithium diffusivity with lithium content in the same $Li_xNi_{0.8}Co_{0.2}O_2$ composition. Saadoune and Delmas[22] reported electronic conductivity for $Li_xNi_{0.8}Co_{0.2}O_2$ exhibiting semiconductor-like behavior. In contrast, Sethuprakhash and Basirun[23] reported metallic-like electronic conductivity for $Li_{1-x}Ni_{0.4}Co_{0.4}Al_{0.2}O_2$.

Thus our objective in this work is to systematically characterize and interpret the transport properties of NCA. We use additive-free, single phase sintered samples in which the extrinsic effects that may be present in composite electrodes are avoided. Using electron blocking and ion blocking cell configurations, respectively, and electrochemical impedance spectroscopy and dc polarization and depolarization techniques (see Table I), we deconvolute the electronic and ionic conductivities of NCA as a function of temperature and Li content.

*Electrochemical Society Active Member
zE-mail: ychiang@mit.edu

Experimental

NCA powder of $Li_{1-x}Ni_{0.8}Co_{0.15}Al_{0.05}O_2$ composition was obtained from NEI Corporation Inc. (Somerset, NJ, USA). Compacted pellets were prepared from the powder by pressing at 340 MPa for 60s, forming cylindrical samples of 14 mm in diameter. The pellets were sintered at 850°C for 12 h in ambient atmosphere, preceded by heating at 5°C/min and cooling at the same rate. This procedure yielded samples of 96–98% relative density, sufficiently high that the measured conductivity represents the bulk value (being proportional to density at high sintered density).

Electrochemical delithiation.— The sintered pellets were polished to a thickness of 0.30 to 0.80 mm. One side of the polished pellets was coated with a thin layer of graphite to form good electrical contact with the metal current collectors in the cells. Delithiation was performed in a Swagelok-type electrochemical cell using lithium metal foil as the counter electrode, the NCA pellet as the working electrode, and a liquid electrolyte mixture containing 1 M $LiPF_6$ in 1:1 by mole of ethylene carbonate/diethyl carbonate (EC/DEC). A Celgard separator (Charlotte, NC, USA) was used to separate the electrodes. A charging current equivalent to C/200 rate was applied using Bio-logic SA France Model: VMP3 (Claix,, France). The current was applied continuously or intermittently (applied for one hour intervals followed by a half-hour rest). After electrochemical delithiation to the desired compositions, the cells were disassembled and the pellets were washed with acetone and pure EC/DEC solvent, and heated at 120°C in an inert atmosphere for at least 24 h in order to homogenize the lithium distribution. The pellets were again polished lightly on both sides to remove any surface lithium salt.

Electronic conductivity measurement.— The as-sintered lithiated and partially delithiated pellets were painted with silver paste on both surfaces forming the cell configuration Ag|NCA|Ag. The pellets were subsequently heated at 120°C overnight in order to remove the organic solvent. The Ag|NCA|Ag cells were placed in battery coin cell holders with support of stainless steel disks on both sides of the pellet. Direct current polarization technique (DC) as well as electrochemical impedance spectroscopy (EIS) were employed to measure the electrical conductivity of the samples using Bio-logic SA France Model: VMP3 (Claix,, France) in the frequency range 200 k Hz–0.5 Hz. The measurements were performed at temperatures from 25–100°C using

Table I. Summary of techniques and cell configurations used to elucidate electronic and ionic conductivity, and the ion diffusivity, as a function of temperature and/or Li-content.

Probed	Technique	Cell configuration	Transport properties as a function of :
Electronic conductivity	EIS - AC	Ag/NCA/Ag	Temperature, Li- content
	EIS - DC	Ag/NCA/Ag	Temperature, Li- content
Ionic conductivity	EIS - AC	Li/PEO/NCA/PEO/Li	Temperature
	EIS - DC	Li/PEO/NCA/PEO/Li	Temperature
Ion diffusivity	EIS - AC and DC	Li/PEO/NCA/PEO/Li	Temperature
	Depolarization	Li/Separator (w. electrolyte)/NCA/current collector	Li- content

Abbreviations: EIS: Electrochemical Impedance Spectroscopy, AC: Alternating Current, DC: Direct Current, GITT: Galvanostatic Intermittent Titration Technique, NCA: $Li_{1-x}Ni_{0.8}Co_{0.15}Al_{0.05}O_2$, PEO: polyethylene oxide.

a VWR temperature controller. The sample temperature was measured by a thermocouple placed near the sample.

Ionic conductivity and diffusivity measurements.— The ionic conductivity and diffusivity of the fully lithiated, starting NCA was measured by direct current polarization (DC) as well as electrochemical impedance spectroscopy (EIS), over the frequency range 200 kHz–10 μHz at AC amplitude 10 mV as a function of temperature. Doped polyethylene oxide (PEO) was used as an electron-blocking, lithium-conducting membrane. The measurements were performed in the symmetric cell configuration Li|PEO|NCA|PEO|Li in a Swagelok-type cell. The PEO membrane was fabricated by mixing PEO powder (from scientific polymer products, Inc., Mw 4,000,000) and LiI (from Aldrich, 99.99%) in a 6:1 molar ratio in dry acetonitrile. Detail of preparation can be found elsewhere.[24]

In order to measure ion diffusivity as a function of lithium content, dc polarization/depolarization measurements were made on thin sintered NCA pellets (0.26–0.30 mm thickness and 0.219–0.158 cm^2 surface area) of known weight, using Swagelok-type cells. The same cell preparation procedure and components as described above for electrochemical delithiation were used. A charging current equivalent to C/400 rate were applied for 25 h, after which the cell was relaxed at open circuit voltage (OCV) conditions for at least 75 h to reach the steady state OCV. Lithium ionic diffusivity was derived from the voltage relaxation vs time (depolarization process). Here we considered the diffusion length to be one half the sample thickness.

X-ray diffraction and rietveld refinements.— Powder X-ray diffraction (PXD) measurements were performed in Bragg-Brentano reflection geometry using a RigakuD/Max/b 185 mm radius goniometer X-Ray Powder Diffractometer equipped with a 13 kW RU300 Cr-source rotating anode X-ray generator (Cr Kα radiation), diffracted beam monochromator and a scintillation point detector. All PXD data were collected from 26 to 120° 2θ with a step size of 0.02° and a step speed of 0.5°/min.

To investigate sample stability during exposure, a sample exposed to ambient air and one stored under inert (glove box) conditions were each analyzed by PXD of the exposed surface. No impurity phases were observed for the latter sample, while for the former sample a relatively large amount of Li_2CO_3 was observed (Figure 1). Therefore, all sample handling and measurements were performed under inert conditions.

To elucidate the change in unit cell parameter in $Li_{1-x}Ni_{0.8}Co_{0.15}Al_{0.05}O_2$ as a function of x, a series of samples was chemically delithiated by reaction with nitroniumtretafluoroborate (Sigma Aldrich) in dry acetonitrile (Alfa Aesar). The reaction mixture was kept in an argon filled glove box for three days in order to complete the reaction. The partially delithiated NCA powder was separated from the solution by centrifugation (Eppendorf Centrifuge, Model 5804R, (Hauppauge, NY, USA)). The powder was washed with additional acetonitrile to remove salt and other impurity phases. The final powder was dried in the glove box at 80°C before PXD measurements.

Rietveld refinements were performed using the program FullProf.[25] The backgrounds were described by linear interpolation between selected points, while pseudo-Voigt profile functions were used to fit the diffraction peaks. In general the unit cell parameters, sample displacement, profile parameters and the overall temperature factors, B_{ov} were refined. The structural model for $Li_{0.99}Ni_{0.71}Co_{0.15}Al_{0.15}O_2$ (space group: R-3m, a = 2.86 and c = 14.199 Å) published by Guilmard et al.[26] was used as starting model for the refinements of $Li_{1-x}Ni_{0.8}Co_{0.15}Al_{0.05}O_2$. The occupancies of Ni and Al were changed to match the material composition while that of Li was changed to accommodate the relevant degree of delithiation. At high degrees of delithiation a second NCA phase was observed, which was satisfactorily modeled using a second R-3m $Li_{1-x}Ni_{0.8}Co_{0.15}Al_{0.05}O_2$ with slightly different cell parameters.

Results and Discussion

Electronic conductivity.— The impedance spectra of as-sintered lithiated NCA measured at selected temperatures on the symmetric cell configuration, Ag|NCA|Ag are shown in Figure 2a. Nearly perfect semicircles are obtained in the temperature range 25–100°C and in the frequency range 2×10^6–5×10^{-2} Hz. The absence of a second semicircle is an indication of absence of other resistive processes and also suggests minor or negligible ionic conductivity. Similar impedance spectra were observed for the partially delithiated samples. The impedance spectra were evaluated with the ideal equivalent circuit shown in Figure 2b. For temperature-dependent measurements, impedances were measured during both heating and

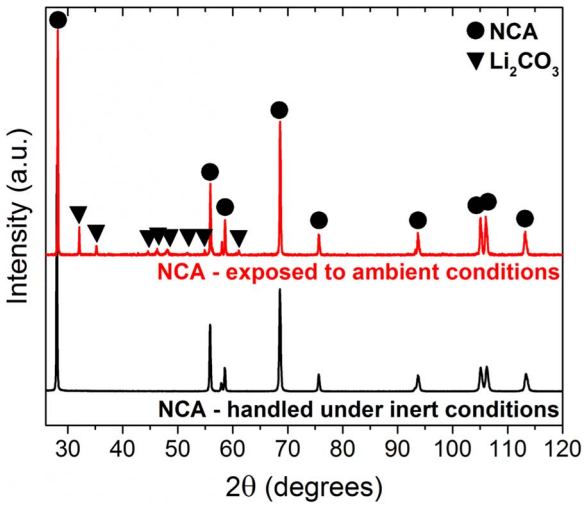

Figure 1. PXD data of NCA samples handled under inert conditions (black curve) and exposed to ambient conditions for 48 h (red curve), respectively. Note that Li_2CO_3 is observed for the sample exposed to ambient conditions, while only peaks from NCA are observed for the sample handled under inert condition.

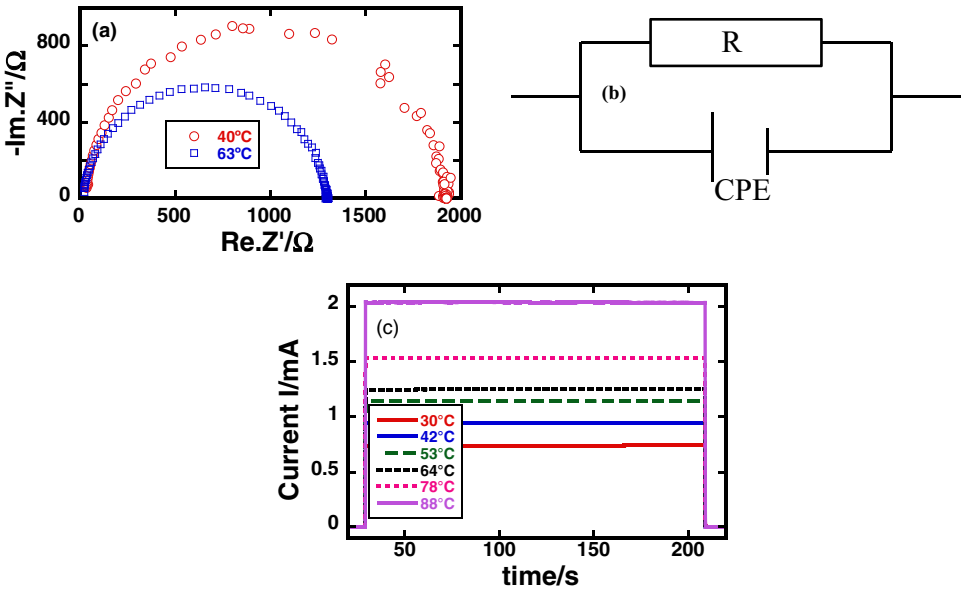

Figure 2. (a) Impedance spectra of as-sintered fully lithiated NCA at two different temperatures measured using the symmetrical cell configuration Ag/NCA/Ag, (b) equivalent circuit used to evaluate the impedance spectra, and (c) time dependent current in polarization measurements performed at various temperatures in the same cell configuration under constant applied voltage.

cooling. The capacitance (C) values can be calculated from the fitting parameters Q and n according to $C = (R^{1-n}Q)^{1/n}$ where Q is a constant phase element and n is essentially a measure of the degree of depression of an arc (here n is usually in the range of 0.98–0.92 depending on the temperature and degree of delithiation). Derived capacitance values are $\sim 10^{-10}$F and thus confirm that the observed impedance responses originate from the bulk (grains) of the samples, i.e. not the grain boundaries.[27] The absence of any additional polarization process (i.e. second semicircle) at low frequencies for all samples indicates that this conduction is predominantly due to electronic carriers. In order to substantiate this observation, DC polarization and depolarization measurements were performed for lithiated and partially delithiated NCA samples using the same cell configuration as for the impedance spectroscopy. Figure 2c is representative of a typical DC measurement on a NCA sample. During application of a constant voltage the current increases in a step-function manner to a stationary value with the applied load and analogously, decays in a step-function on switching off the applied voltage. Such behavior is indicative of a electronically dominated conduction process since in the case of significant contributions from ionic motion, a continuous increase of the current during polarization limited by a steady state situation, and a symmetrical decay of the current during depolarization with rate constants being determined by lithium diffusion D^{δ}_{Li} are expected.[28–30]

The electronic conductivities of the lithiated and partially delithiated NCA are plotted in Figure 3a as a function of inverse of temperature. The conductivities of the partially delithiated samples measured at a given temperature increase monotonically with increasing delithiation (Figure 3b, for measurements at 30°C). Over the measured compositional range, the electrical conductivity shows thermally-activated behavior. The values of activation energy, calculated using an Arrhenius law, varies from 0.22–0.14 eV (±0.04 eV) as shown in Figure 3a, and is consistent with the value reported by Saadoune and Delmas[22] for $Li_xNi_{0.8}Co_{0.2}O_2$. These are typical values for the migration process of a small polaron generally observed in mixed-valence systems.[31] It is reported that Co is less prone to oxidize from the trivalent to tetravalent state in the presence of Ni.[32] The electronic configurations of Co^{3+}, $Ni^{3+}$and Ni^{4+} have the (t_2) orbital filled in each case. As a result, electron delocalization is unlikely. The increase in electronic conductivity is associated with the presence of mixed Ni^{3+}/Ni^{4+} valence states resulting from delithiation, which leads to hole formation in the narrow (Ni^{4+}/Ni^{3+}) band. It is seen from the Figure 3a and 3b that beyond 60% delithiation (i.e. x = 0.60) the sample exhibits a sharp rise in electronic conductivity. This may be due to oxidization of cobalt from the trivalent to tetravalent state at this delithiation level. The degree of cobalt oxidation is evidently small, since a high degree of oxidation would lead to metallic behavior due to the presence of holes in the broad t_2 band. We were not able to measure the electronic

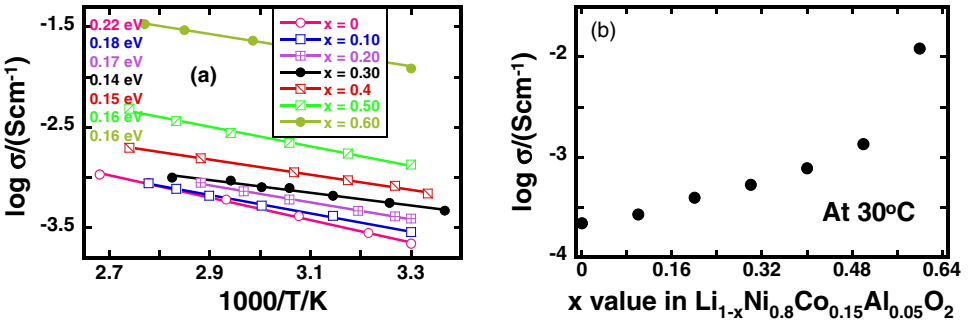

Figure 3. (a) The electronic conductivity of lithiated and partially delithiated NCA ($Li_{1-x}Ni_{0.8}Co_{0.15}Al_{0.05}O_2$) (as a function of inverse temperature obtain from DC measurement and calculated activation energy using the Arrhenius equation. AC impedance also exhibit the same magnitude of conductivity. (b) The electronic conductivity of NCA ($Li_{1-x}Ni_{0.8}Co_{0.15}Al_{0.05}O_2$) as a function of x in $Li_{1-x}Ni_{0.8}Co_{0.15}Al_{0.05}O_2$ at 30°C obtained from DC measurement.

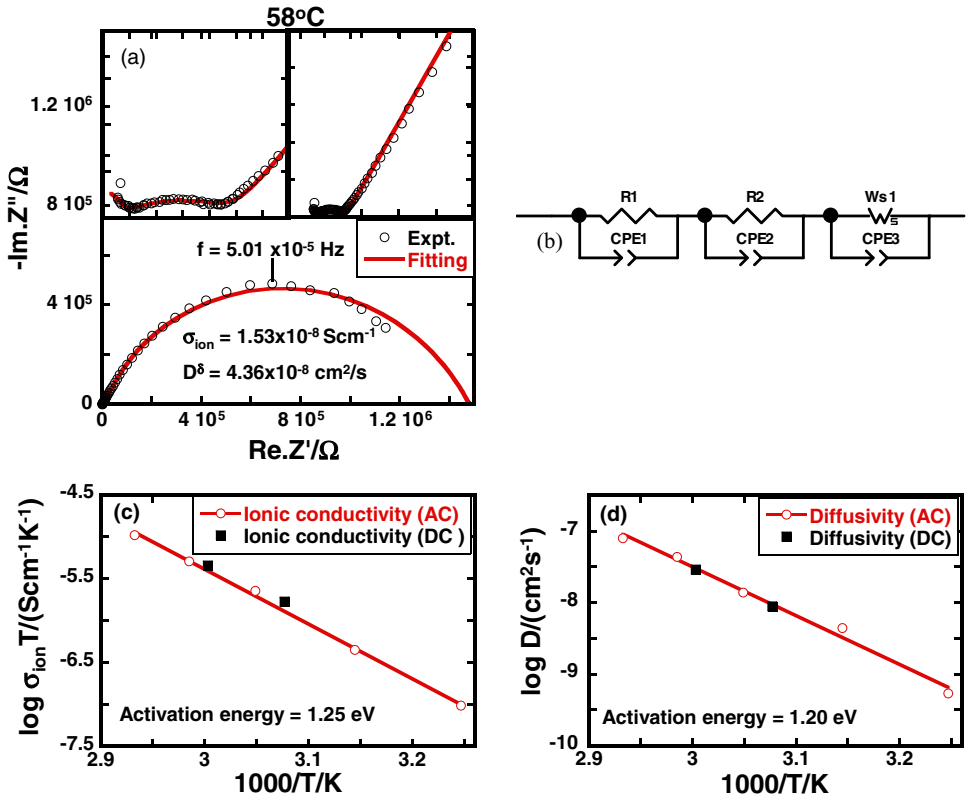

Figure 4. (a) Impedance spectra of NCA obtained from the electron blocking cell configuration Li/PEO/NCA/PEO/Li at 58°C. Inset shows the magnification of high frequency spectra. (b) Equivalent circuit used to fit the impedance spectra. (c) Product of ionic conductivity and temperature of fully-lithiated NCA as a function of inverse temperature obtained from AC and DC measurements on the electron blocking cell Li/PEO/NCA/PEO/Li. (d) Ionic diffusivity of lithiated NCA as a function of inverse temperature obtained from AC and DC measurements on the electron blocking cell.

conductivity beyond 60% delithiation, as the samples were too fragile for reliable assembly of cells. Comparing to literature, Sethuprakhash and Basirun[24] reported metallic-like electronic conductivity of lithiated $Li_{1-x}Ni_{0.4}Co_{0.4}Al_{0.2}O_2$. This is surprising if their samples are truly lithiated to a high extent (low Co^{3+}/Co^{4+} ratio).

Ionic conductivity and diffusivity by AC impedance.— Results with electron-blocking cells must take into account the temperature dependent ionic conductivity of the PEO blocking layer. Figure 4a shows the impedance spectra of lithiated NCA measured at 58°C in the cell configuration Li/PEO/NCA/PEO/Li. In contrast to the ion-blocking cells above, these impedance spectra consist of two semicircles at high frequencies (inset of Figure 4a) followed by a Warburg response at low frequencies. The high frequency semicircle represents the total resistance to electronic and ionic motion including contributions from the bulk conductivity of PEO. The Warburg response is indicative of stoichiometric polarization owing to blocking of electrons. In order to obtain the ionic conductivity and diffusivity, the impedance spectra were fitted with the equivalent circuit as shown in Figure 4b. Good agreement is obtained between the simulated and experimental data. Qualitatively similar impedance spectra were observed for other temperatures; however, at temperatures below 35°C the frequency range is not sufficiently wide to obtain the relaxation frequency. Hence, for the lower temperatures, the model fit to lower frequencies was extrapolated to reach the relaxation frequency. The ionic conductivity and diffusivity respectively are plotted against inverse temperature in Figure 4c and 4d, the diffusivity being obtained via the Nernst-Einstein relation. An Arrhenius relationship is obtained, with the activation energies for ionic conductivity and diffusivity being 1.25 ±0.2 and 1.20 ± 0.2 eV, respectively. This is to our knowledge the first measurement of these ion transport parameters for any NCA composition. The obtained activation energies are comparable to those for other lithium ion cathode compounds.[33,34] Given predominant electronic conductivity, the Li^+ diffusivity (D_{Li}) should have the form $D_{Li} \propto \sigma_{ion}(\frac{x_{ion}}{C_{ion}} + \frac{x_{eon}}{C_{eon}})$ where x_{ion} and x_{eon} refer to the contributions due to trapping of ionic and electronic carriers and c_{ion}, c_{eon} denote to the ionic and electronic carrier concentrations.[35] It is discernable from Figure 4c and 4d that both the ionic conductivity and diffusivity display single slope behavior which indicates the absence of charge carrier trapping effect (x_{ion} and x_{eon}). That is, charge carrier association-dissociation is not prominent in the measured temperature range. In the intrinsic dilute defect, $c_{ion} \gg 1$, the ionic diffusivity should be higher than the ionic conductivity according to above equation, as is observed in Figure 4c and 4d.

Ionic conductivity and diffusivity by steady state polarization/depolarization.— DC polarization/depolarization measurements were also performed using electronically blocking cell arrangements over a range of temperatures in order to substantiate the result obtained from the impedance measurements. These measurements were not performed at low temperature due to the excessively long times required to reach steady state (also observed in AC impedance). Figure 5 shows the time dependence of the polarization voltage (galvanostatic mode). The voltage immediately jumps from zero to $IR_{el}R_{ion}/(R_{el} + R_{ion})$ where R_{ion} and R_{el} are the resistances due to Li ion and electronic carriers. With increasing time, the partial current of the blocked electrons decreases and eventually vanishes. A steady state is then observed (voltage being IR_{ion}) during which the total current is carried only by the non-blocked ions. The relaxation time of the polarization process is τ^δ, which provides the chemical diffusion coefficients D^δ_{Li} (via $\tau^\delta = L^2/(\pi^2 D^\delta_{Li})$. It should be noted that owing to the internal concentration profiles, σ_{ion} and D^δ_{Li} are averaged over a Li composition range, corresponding to a polarization voltage of 50 mV. The behavior of the depolarization was analogous to that during

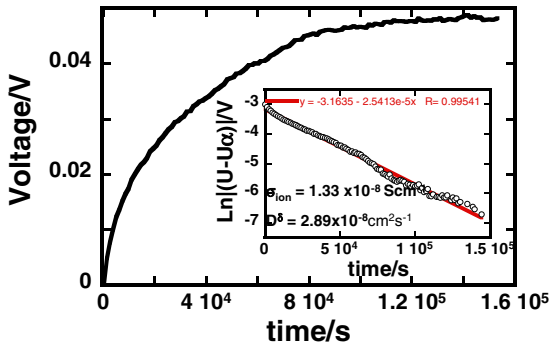

Figure 5. Time dependent DC polarization voltage at ~60°C obtained from the electron blocking cell Li/PEO/NCA/PEO/Li. Results are fitted with Eq. 1 in order to obtain ionic conductivity and diffusivity (inset).

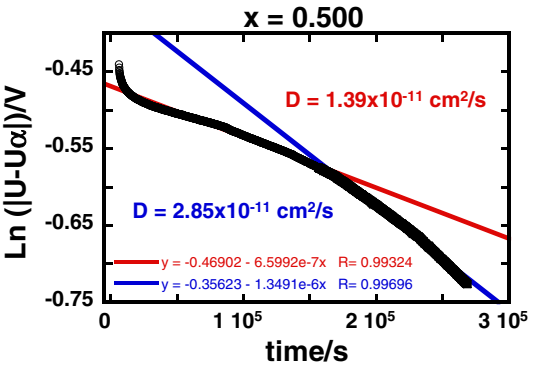

Figure 7. Fitting the depolarization cell voltage at point $x = 0.5$ of Figure 6a with Eq. 1 in order to extract the chemical diffusivity. Two slopes are clearly fitted.

polarization. Owing to the relatively high diffusion coefficients, a steady state cell voltage was reached during polarization at ~60°C. As the long-time polarization voltage ($t > \tau^{\delta}$) depends on time according to[28–30]:

$$U_{ion} = [(i_p L)/\sigma] + \left(\frac{\sigma_{el}}{\sigma}\right)\left[\frac{i_p L}{\sigma_{ion}}\right]\left\{1 - \left(8/\pi^2\right) exp\left[-\left(\frac{t}{\tau^{\delta}}\right)\right]\right\} \quad [1]$$

A plot of $\ln|U(t)\text{-}U(t=\infty)|$ vs. t should generate a straight line with a slope of $\tau^{\delta} \propto (\frac{1}{D_{Li}^{\delta}})$. Diffusivity and ionic conductivity data derived from the DC measurement are compared in Figure 4c and 4d with the AC data, and the two are in good agreement.

Lithium ion diffusivity from depolarization.— Figure 6a shows the cell voltage vs. time during the stepwise galvanostatic titration of fixed amounts of lithium from the NCA sample. A lithium concentration gradient is developed across the sample during titration. After each delithiation step, the cell is allowed to relax in the OCV condition, and the cell voltage slowly reaches steady state, corresponding to removal of the lithium concentration gradient. Lithium ion diffusivity data derived from the relaxation of the cell voltage, i.e. the depolarization process, using Eq. 1 is shown in Figure 6b. It is seen that the depolarization cell voltage can be fitted very well with Eq. 1. However, at 50% delithiation ($x = 0.50$), a change in the slope of the depolarization curve was observed after ~1.5×10^5 s (Figure 6a). The two slopes can be fitted separately by Eq. 1 and clearly shows two regimes, as shown in Figure 7. The change in the depolarization rate may originate either from the formation of a second phase during delithiation, or a change in the diffusion mechanism.

To investigate this observation further, we prepared a series of chemically delithiated NCA powders and performed X-ray diffraction measurements, for which results appear in Figure 8. For $x = 0.0$ and 0.1, only one NCA phase was observed (denoted NCA1), while for samples of $x \leq 0.25$ a second NCA phase (denoted NCA2) was also observed. As the lithium content is decreased ($x = 0.25$ to 0.5), the fraction of NCA2 increases from 5 to 14 mol%, while further decrease ($x = 0.75$) results in only a slight increase in the amount of NCA2 to 15 mol%. Thus the amount of NCA2 reaches a plateau value. The *R-3m* symmetry of NCA1 is preserved in NCA2, but the cell parameters are different for NCA2, and suggest a significantly different Li-content in this phase. A notable feature for both phases is the appearance of a maximum in unit cell dimensions at $x = 0.5$, which suggests a change in cation ordering at that composition. Yoon et al.[38] have previously reported similar structure observations for NCA using in situ electrochemical cells, wherein after initial delithiation a second NCA phase appears exhibits a maximum in *c*-axis and minimum in *a*-axis with increasing *x*. However, there are significant differences between the present results and theirs, in the relative amounts of the two phases as a function of *x*, the concentrations at which the maximum in *c* and minimum in *a* occur, and the fact that in our case, both phases exhibit the same variation in *c* and *a* dimensions with *x*, whereas in their work one of the phases exhibits nearly invariant c and a.

The room-temperature lithium ion diffusivity obtained from depolarization measurements are plotted in Figure 9 as a function of lithium content. Firstly, note that the ionic conductivity varies by about an order of magnitude with *x*, and is everywhere at least 10^5 lower than the electronic conductivity (Figure 3b). Secondly, the ionic conductivity shows an inverse relationship to the unit cell parameters in Figure 8b, whereby diffusivity decreases as unit cell dimensions increase. The minimum in diffusivity at $x = 0.5$ corresponds to a maximum in unit cell dimensions at the same composition. This is surprising, and is

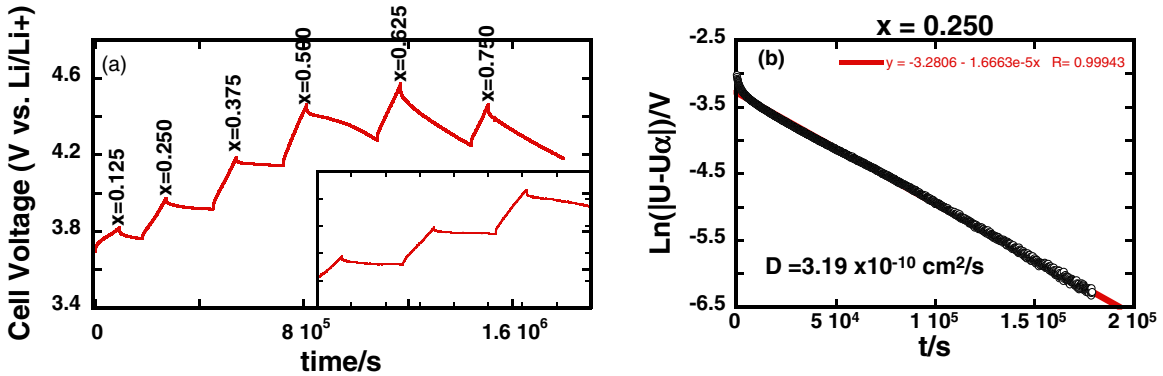

Figure 6. (a) Time dependent cell voltage measured on the NCA ($Li_{1-x}Ni_{0.8}Co_{0.15}Al_{0.05}O_2$) plate by titrating a fixed amount of lithium and holding at open circuit conditions. (b) Fit of the depolarization cell voltage to Eq. 1 in order to extract the chemical diffusivity of lithium ion at $x = 0.25$.

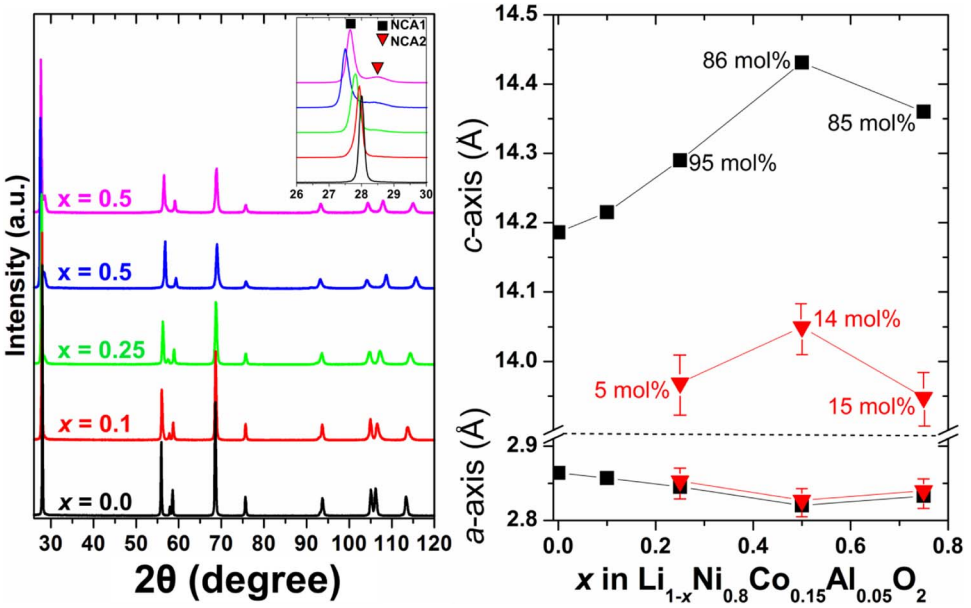

Figure 8. Left: PXD data for chemical delithiated $Li_{1-x}Ni_{0.8}Co_{0.15}Al_{0.05}O_2$. The inset shows the 2theta region around the (003) reflection. Note the appearance the (003) peak of the second NCA phase (denoted NCA2) at $x = 0.25$. Right: Unit cell parameters (a- and c-axis) of the two observed NCA phases (NCA1: black squares, NCA2: red triangles). The mol% of the two phases for each x is noted in plot. Error bars for NCA1 fall within symbols.

counter to the expectation that a c-axis expansion corresponding to an increase in the Li slab distance lowers the activation energy for migration and should therefore increase the Li diffusion coefficient.[36,37] Recalling that the depolarization data (Figure 6b) indicate a change in mechanism and/or rate-controlling phase around $x = 0.5$, we considered alternative explanations. We examined the diffraction data for evidence for changes in cation ordering. Rietveld refinement did not indicate significant mixing between Li and the transition metals. Possible changes in cation ordering within the transition metal layers need to be investigated further. No superstructure peaks indicative of ordering were detected. The dependence of ion diffusivity on Li vacancy concentration x is consistent with a defect chemical model where between $x = 0$ and $x = 0.5$, diffusivity is dependent on interstitial concentration and therefore decreases with increasing vacancy concentration through a Frenkel equilibrium. The increase in diffusivity for $x > 0.5$ is consistent with a dependence on vacancy concentration. However, changes in cation ordering which are more subtle than can be detected in the present diffraction data, and related changes in migration energy, may be the dominant influence.

We know of no other published diffusion data for NCA to compare with the present results. For NC, however, Montoro et al.[21] reported a M-shaped relation between the chemical diffusion coefficient of $Li_xCo_{0.5}Ni_{0.5}O_2$ and lithium content, based on GITT measurements of

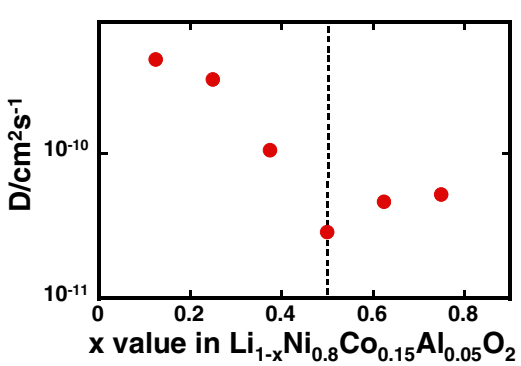

Figure 9. Diffusivity of NCA ($Li_{1-x}Ni_{0.8}Co_{0.15}Al_{0.05}O_2$) as a function of lithium content at room temperature obtained from depolarization experiments shown in Figure 6a.

Table II. Diffusivity of NCA at 30°C measured by different techniques and comparison with the available literature data of NC.

Technique Used	Composition	Diffusivity (cm^2/s)	Reference
AC	$LiNi_{0.8}Co_{0.15}Al_{0.05}O_2$ (NCA)	$\sim 3\times10^{-10}$	This study
DC	$LiNi_{0.8}Co_{0.15}Al_{0.05}O_2$ (NCA)	$\sim 2\times10^{-10}$	This study
Depolarization	$Li_{0.875}Ni_{0.8}Co_{0.15}Al_{0.05}O_2$ (NCA)	$\sim 4\times10^{-10}$	This study
GITT	$Li_{0.9}Ni_{0.5}Co_{0.5}O_2$ (NC)	$\sim 10^{-10}$	22
GITT	$Li_{0.9}Ni_{0.8}Co_{0.2}O_2$ (NC)	$\sim 10^{-8}$	21

composite electrodes. The diffusivity data reported by Montoro ranged from $\sim 10^{-10}$ to $\sim 5 \times 10^{-9}$ cm^2s^{-1} over the entire Li-compositional window. In contrast, Cho et al.[20] reported an almost constant lithium diffusion coefficient of $Li_xNi_{0.8}Co_{0.2}O_2$ as a function of lithium content. However, their data showed a much higher diffusivity ($\sim 10^{-8}$ cm^2s^{-1}). We believe that extrinsic factors may be present in these previous results due to the nature of the samples, and that neither may represent the pure single phase transport behavior. Table II compares the diffusivity data obtained in the present work with literature results.

Conclusions

Electronic and lithium ionic transport in NCA have been measured using ion and electron blocking cell configurations and both ac and dc techniques. NCA exhibits semiconducting behavior over the entire range of lithium concentrations measured ($x = 0.0$ to 0.7). Starting from the fully lithiated state, the electronic conductivity gradually increases with increasing delithiation, and rises more sharply beyond about 60% delithiation. We suggest that the latter increase is due to the onset of Co^{3+}/Co^{4+} multivalency. Regarding lithium ionic conductivity (and diffusivity), in fully lithiated NCA the activation energy is 1.25 eV. No evidence for charge carrier association or dissociation was seen in the measured temperature range. However, the ion diffusivity as a function of lithium concentration shows V-shaped behavior

with a minimum at about $x = 0.5$. The unit cell parameters show the opposite trend with a maximum at $x = 0.5$. This behavior is counter to expectations for ion migration energy as a function of *c*-axis dimensions, and suggests more subtle cation ordering effects that remain to be resolved. From the magnitude of the electronic and ionic transport parameters across the measured range of Li concentration, it can also be concluded that chemical diffusion is always limited by lithium ion transport rather than electronic conductivity, and that bulk transport is rapid enough to allow charging and discharging of micron size particles at practical C-rates regardless of state-of-charge.

Acknowledgments

For this work R. A. and Y.-M. C. were supported by the Assistant Secretary for Energy Efficiency and Renewable Energy, Office of Vehicle Technologies of the U. S. Department of Energy under Contract No. DE-AC02-05CH11231, Subcontract No. 7056592 under the Advanced Battery Materials Research (BMR) Program, and subsequently supported by NECCES, an Energy Frontier Research Center funded by the U. S. Department of Energy, Office of Science, Office of Basic Energy Sciences under Award Number DE-SC0001294. DBR was supported by DOE project number DE-SC0002626. DBR also acknowledges fellowship support from the Carlsberg Foundation.

References

1. V. k. Etacheri, R. Marom, R. Elazari, G. Salitra, and D. Aurbach, *Energy Environ. Sci.*, **4**, 3243 (2011).
2. J. Cabana, H. Zheng, A. K. Shukla, C. Kim, V. S. Battaglia, and M. Kunduraci, *J. Electrochem. Soc.*, **158**, A997 (2011).
3. R. Koksbang, J. Barker, H. Shi, and M. Y. Saidi, *Solid State Ionics*, **84**, 1 (1996).
4. J. L. Lei, F. McLarnon, and R. Kostecki, *J. Phys. Chem. B*, **109**, 952 (2005).
5. A. D. Epifanio, F. Ronci, V. R. Albertini, E. Traversa, and B. Scrosati, *Phys. Chem. Chem. Phys.*, **3**, 4399 (2001).
6. C. H. Lu and H. C. Wang, *J. Mater. Chem.*, **13**, 428 (2003).
7. A. Kinoshita, K. Yanagida, A. Yanai, Y. Kida, A. Funahashi, T. Nohma, and I. Yonezu, *J. Power Sources*, **102**, 283 (2001).
8. A. Ueda and T. Ohzuku, *J. Electrochem. Soc.*, **141**, 2010 (1994).
9. J. Cho, G. Kim, and H. S. Lim, *J. Electrochem. Soc.*, **146**, 3571 (1999).
10. C. C. Chang, N. Scarr, and P. N. Kumta, *Solid State Ionics*, **112**, 329 (1998).
11. R. V. Chebiam, F. Prado, and A. Manthiram, *J. Electrochem. Soc.*, **148**, A49 (2001).
12. H. Watanabe, T. Sunagawa, H. Fujimoto, N. Nishida, and T. Nohma, *Sanyo Tech. Rev.*, **30**, 84 (1998).
13. T. Ohzuku, T. Yanagawa, M. Kouguchi, and A. Ueda, *J. Power Sources*, **68**, 131 (1997).
14. Y. Nitta, K. Okamura, K. Haraguchi, S. Kobayashi, and A. Ohta, *J. Power Sources*, **54**, 511 (1995).
15. B. Banov, J. Bourilkov, and M. Mladenov, *J. Power Sources*, **54**, 268 (1995).
16. Y. Nishida, K. Nakane, and T. Satoh, *J. Power Sources*, **68**, 561 (1997).
17. H. Arai, S. Okada, Y. Sakurai, and J. Yamaki, *J. Electrochem. Soc.*, **144**, 3117 (1997).
18. Y. Gao, M. V. Yakovleva, and W. B. Ebner, *Electrochem. Solid State Lett.*, **1**, 117 (1998).
19. Y. Zhangand and C.-Y. Wang, *J. Electrochem. Soc.*, **156**(7), A527 (2009).
20. J. Cho, H. S. Jung, Y. C. Park, G. Kim, and H. S. Lim, *J. Electrochem. Soc.*, **147**(1), 15 (2000).
21. L. A. Montoro and J. M. Rosolen, *Electrochimica Acta*, **49**, 3243 (2004).
22. I. Saadoune and C. Delmas, *J. Solid State Chem.*, **136**, 15 (1998).
23. V. Sethuprakhash and W. J. Basirun, *Materials Resaerch Innovation*, **15**, 91 (2011).
24. Y. Liu, S. Gorgutsa, C. Santato, and M. Skorobogatiy, *J. Electrochem. Soc.*, **159**(4) A349 (2012).
25. R. Carvajal, *J. Physica B*, **192**, 55 (1993).
26. M. Guilmard, C. Pouillerie, L. Croguennec, and C. Delmas, *Solid State Ionics*, **160**, 39 (2003).
27. F. S. Baumann, PhD thesis, "Oxygen reduction kinetics on mixed conducting SOFC model cathodes" Stuttgart University press, 2006, page 33.
28. C. Wagner, *Proc. 7th Meeting Int. Comm. on Electrochem. Thermodynamics and Kinetics, Lindau 1955*, Butterworth, London, (1957).
29. I. Yokota, *J. Phys. Soc. Japan.*, **16**, 1961 (2213).
30. J. Maier, *Physical Chemistry of Ionic Materials: Ions and Electrons in Solids*, Wiley, Chichester, (2004).
31. T. Maxisch, F. Zhou, and G. Ceder, *Physical Review B*, **73**, 104301, (2006).
32. D. Carlier, M. Menetrier, and C. Delma, *J. Mater. Chem.*, **11**, 594 (2001).
33. R. Amin, J. Maier, P. Balaya, D. P. Chen, and C. T. Lin, *Solid State Ionics.*, **178**, 1683 (2008).
34. A. K. Ivanov-Shitz, V. V. Kireev, O. K. Mel'nikov, and L. N. Demianets, *Crystallography Report*, **46**, 864 (2001).
35. J. Maier, *J. Am. Ceram. Soc.*, **76**, 1212 (1993).
36. A. Van der Ven and G. Ceder, *Electrochem. and Solid State. Lett.*, **3**(7), 301 (2000).
37. K. Kang and G. Ceder, *Phys. Rev. B*, **74** (9), 094105 (2006).
38. W.-S. Yoon, K. Y. Chung, J. McBreen, and X.-Q. Yang, *Electrochemistry Comm.*, **8**, 1257 (2006).

Journal of The Electrochemical Society, **162** (7) X15-X15 (2015)
0013-4651/2015/162(7)/X15/1/$33.00 © The Electrochemical Society

Erratum: Characterization of Electronic and Ionic Transport in $Li_{1-x}Ni_{0.8}Co_{0.15}Al_{0.05}O_2$ (NCA) [*J. Electrochem. Soc.*, 162, A1163 (2015)]

Ruhul Amin,[a] Dorthe Bomholdt Ravnsbæk,[a,b] and Yet-Ming Chiang[a]

[a]*Department of Materials Science and Engineering, Massachusetts Institute of Technology (MIT), Cambridge, Massachusetts 02139, USA*
[b]*Department of Physics, Chemistry and Pharmacy, University of Southern Denmark (SDU), 5320 Odense M, Denmark*

On page A1169, left column the text beneath the Acknowledgments heading should be

For this work R. A. and Y.-M. C. were supported by the Assistant Secretary for Energy Efficiency and Renewable Energy, Office of Vehicle Technologies of the U. S. Department of Energy under Contract No. DE-AC02-05CH11231, Subcontract No. 7056592 under the Advanced Battery Materials Research (BMR) Program, and subsequently supported by NECCES, an Energy Frontier Research Center funded by the U. S. Department of Energy, Office of Science, Office of Basic Energy Sciences under Award Number DE-SC0012583. DBR was supported by DOE project number DE-SC0002626. DBR also acknowledges fellowship support from the Carlsberg Foundation.